TREATMENT OF MINE WASTEWATER
USING ACTIVATED CARBON PREPARED FROM WASTE PINE
SAWDUST IN ZAMBIA

Student No.: 18M53078 Name: Abednego SHAMBWEKA
Supervisors: Ryuichi EGASHIRA, Hiroaki HABAKI

1. Introduction

Rapid industrialization and increase in human population has led to increase in environment pollution, which for many developing countries, has remained a challenge to control. In particular, Zambia's Copperbelt province, the country's hub of industrial activity has been facing two major environmental challenges. The first challenge is mine wastewater pollution containing high concentration of heavy metals that are harmful to human health [1]. The second problem is presence of huge piles of unutilized sawdust, from sawmill industry, that are disposed of by open dumping. Open dumping of sawdust reduces trading space and contribute to greenhouse gas emission [2]

According to Mukosha *et al.* [3], the conventional mine wastewater treatment technology of chemical precipitation has problems of incomplete precipitation and generation of toxic voluminous sludge that lead to secondary environmental pollution. Other advanced wastewater treatment technologies such as solvent extraction, ion exchange, reverse osmosis etc. are expensive to apply. For this reason, there is growing interest in the use of low-cost adsorbents from various biomass materials to produce activated carbon for treatment of mine wastewater. Examples of such adsorbents include, palm oil shells, coconuts shells, corn cobs and pine tree sawdust. The latter is the most attractive for Zambia due to its abundancy.

This study aims to solve the local problem of heavy metal pollution in mine wastewater on the Copperbelt province mines using activated carbon prepared from locally abundant Pine Sawdust (PSD). This will be accomplished by first characterizing the PSD followed by preparation of activated carbon and finally ending with batch adsorption studies of the target heavy metals, copper and cobalt.

2. Materials and Methods

2.1. Characterization of Zambian pine sawdust

Pine sawdust (PSD) samples were obtained from a local company, Baraka Sawmill Company limited, situated in the city of Ndola on the Copperbelt Province of Zambia. The samples were washed several times with distilled water to remove surface impurities followed by drying for 24hrs at 383K in an oven. The samples were then sieved to between 0.212-1.0 mm. Ultimate and proximate analyses were conducted using procedure previously used [4] while thermogravimetric analysis was done using. thermogravimetric analyser (DTG-60H, Shimadzu Corp)

and based on analysis conditions shown in **Table 1**.

2.2. Preparation of activated carbon

Phosphoric acid solution (H_3PO_4) from wako pure chemicals industries limited was used to prepare various concentration of H_3PO_4 (C_p) ranging from 1-8 kmol m^{-3}. 0.01kg of PSD sample was chemically treated with the prepared solutions for 6hrs at 358K. The sample was then dried overnight in an oven at 383K and later thermally treated in an electric furnace using experimental conditions stated in **Table 2**, to finally produce activated carbon (AC).

2.3. Batch equilibrium adsorption studies

Batch adsorption studies were conducted using single solute aqueous solutions of Cu^{2+} and Co^{2+} prepared from $CuSO_4 5H_2O$ and $CoSO_4 7H_2O$ respectively. 5 x10^{-5}m^3 Erlenmeyer flasks, thermostatic shaker water bath and concentration analyser ICP-AES (SPS7800 Series, Seiko Instruments Inc.) were used in the batch adsorption studies based on conditions shown in **Table 3**.

Table 1 Thermogravimetric analysis conditions

Feed	PSD
Mass of feed [kg]	1×10^{-5}
Particle size [m]	$< 2.12\times10^{-6}$
Initial temperature [K]	303
Final temperature [K]	1273
Thermogravimetric treatment time [h]	0.5
N_2 flow rate [m^3 h^{-1}]	9.0×10^{-3}

Table 2 Thermal treatment conditions

Feed	H_3PO_4 treated PSD
Thermal treatment temperature, T [K]	673- 1073
Thermal treatment time, t [h]	0.5 - 2

Table 3 Batch equilibrium adsorption conditions

Volume of aqueous solution at initial, V_o [m^3]	2.5×10^{-5}
Initial concentration of aqueous solution, $C_{i,0}$ [kmol m^{-3}]	$1.0-23 \times10^{-3}$
Mass of activated carbon, S_{AC}, [kg]	1×10^{-4}
Contact time, t_c [h]	240
Water bath temperature, T_{wb} [K]	300
Speed of shaker, f [strokes h^{-1}]	600

3. Results and discussion
3.1. Characterization of Zambian pine sawdust

Ultimate and Proximate analyses of PSD are shown in **Table 4**. The PSD used in this study had high carbon necessary for production of high yield AC. The results were similar to those found using same precursor by Gao *et al.* [5].

Figure 1 shows the thermalgravimetric analysis profile of PSD in which the mass ratio of the carbon, Ms, was defined as,

$$M_s = S_{TGA}/S_{PSD} \qquad (1)$$

A decrease in the mass ratio of about 0.06 took place as temperature increased from 303-393K. This represented loss of moisture from PSD. The second change was loss of volatile matter with approximate mass ratio of 0.72 corresponding to temperature range 303-393K and finally formation of carbon starting from around 670K. The later indicated carbonization temperature for PSD.

Table 4 Ultimate and proximate analyses of PSD

	This study	Gao et al. (2018)
C	0.47	0.49
O*	0.46	0.44
H	0.06	0.06
N	0.001	0.003
S	-	-
Moisture	0.05	0.09
Fixed Carbon*	0.14	0.14
Volatile Matter	0.80	0.75
Ash	0.001	0.006

All values are on mass ratio [-] basis, * obtained by difference from sum of mass ratio
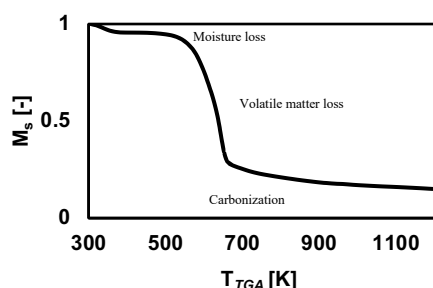
Fig. 1 Thermogravimetric analysis profile for raw PSD

### 3.2. Characterization of activated carbon

The yield, Y, of AC was defined as

$$Y = S_{AC}/S_{PSD} \qquad (2)$$

Figures 2, 3 and **4** show the effect C_p, T and t on Y. In all cases, the yield initially increased and later reduced. The reason for the initial increase in the yield was due to the formation of polymers containing phosphate and polyphosphate bridges. This led to increase in the material mass that resulted in increase of yield. Around 2kmol m^{-3}, enhanced hydration reactions took place resulting in mass loss which resulted in reduction of yield. In the case of Figures 3 and 4, increased T and t, led to increased volatisation that led to division of bonds of the carbon-phosphoric acid polymer. These broken polymers eventually volatilised leading to low yield [6].

Figures 5, 6 and **7** show the effect of C_p, T and t on the specific surface area (A) and micropore volume (V_{mp}). With increase in C_p, A and V_{mp} increased to attain a maximum of $1718\times 10^3 m^2$ kg^{-1} and $0.92\times 10^{-3}m^3$ kg^{-1} respectively, before finally reducing. This was also the case involving variation of T. In Figure 4, Y reduced as t increased. As C_p increased, the amount of H_3PO_4 that remained incercalated in the internal structure of the PSD also increased leading to increased polymer formation of H_3PO_4 with carbon in the PSD. The formation of these polymers was accompanied with enhanced gas evolution that led to the initial increase in A and V_{mp}. Above 2kmol m^{-3} (Figure 2) or 873K (Figure 3), excess hydration and volatisation weakened the cross-linked structure of carbon-phosphoric acid. This led to collapsing of the structure and consequently reduction in A and V_{mp} [6,7].
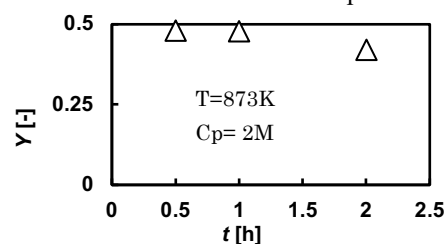
In Figure 3, increase in t, resulted in more gaseous evolution from volatisation reactions. This resulted in increase in A.
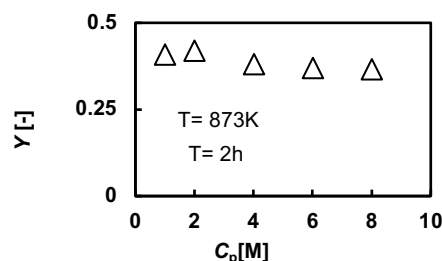
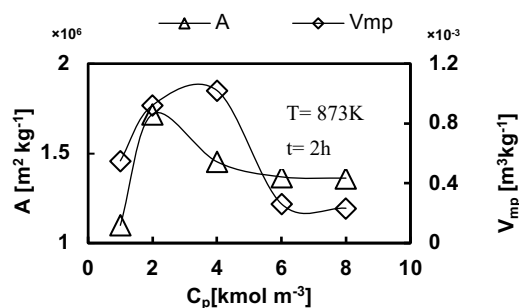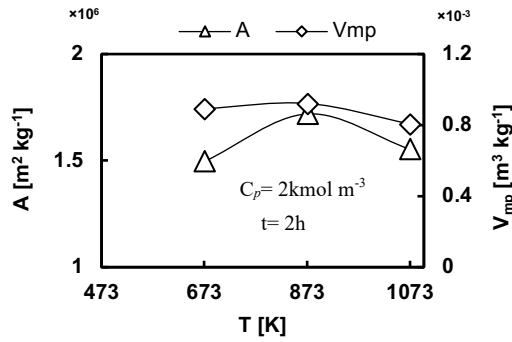**Fig. 2** Effect of H_3PO_4 concentration on yield
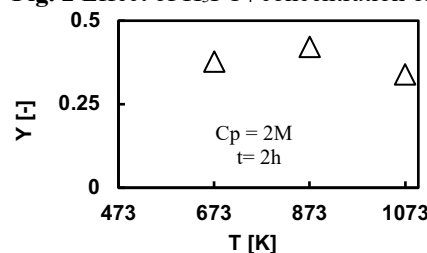
Fig. 3 Effect of thermal treatment temperature on yield
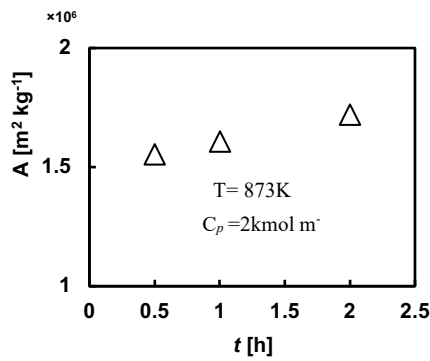

Fig. 4 Effect of thermal treatment time on yield

Fig. 5 Effect of H_3PO_4 concentration on AC surface area and micropore volume.
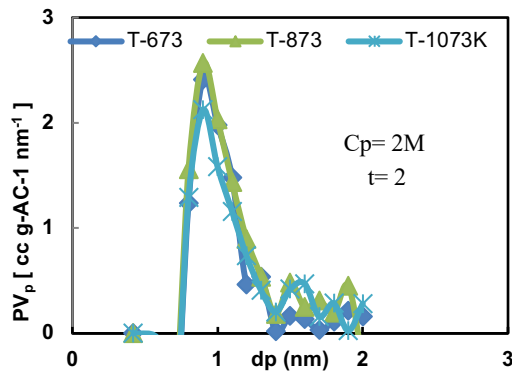
Fig. 6 Effect of thermal treatment temperature on AC surface area and micropore volume

Fig. 7 Effect of thermal treatment time on AC surface area

Figure 8 shows the pore size distribution of AC obtained by varying T. The highest proportion of pore volume was attained with pore diameter between 0.75 to 1.4nm. Pore development increased as T increased then later reduced. This is because the initial increase in T promoted gas evolution that resulted in increased porous structure development. At 1073K, the structure collapsed due to excessive temperature. This resulted in reduced pore structure development. The significance of this results is that the pore width developed was higher than the target ions whose hydrated radii are 0.419 and 0.423nm for Cu^{2+} and Co^{2+} respectively. The developed pores were suitable for adsorption of the target ions.

Fig. 8 Effect of Thermal treatment temperature on pore size distribution of AC

3.3. Batch equilibrium adsorption studies

The amount of metal ion adsorbed on AC, q_i, was calculated from material balance relationship,

$$V_0 C_{i,0} = V_0 C_i + S q_i \qquad (3)$$

The fractional removal of ions, Y_i, was defined as,

$$Y_i = (C_{i,0} - C_i)/C_{i,0} \qquad (4)$$

Adsorption analysis was done using Langmuir model,

$$q_i = q_i^* K_{L,i} C_i / (1 + K_{L,i} C_i) \qquad (5)$$

Five kinds of AC samples were used in adsorption study as listed in Table 5.

Results of fractional removal are shown in **Figure 9** using AC 2. Y_i decreased with increase in initial metal concentration. The fractional removal of Cu^{2+} was generally higher than that of Co^{2+}.
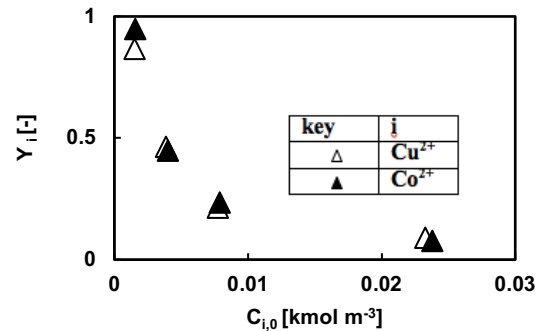
Fig. 9 fractional removal of Cu^{2+} and Co^{2+}

Figure 10 shows adsorption isotherms of Cu^{2+} and Co^{2+} on AC 2. The adsorption isotherms of these ions followed Langmuir model with saturated adsorbed amounts of 5.16 x 10 $^{-4}$ and 4.44 x10^{-4} kmol Kg^{-1} for Cu^{2+} and Co^{2+} respectively. The difference in the adsorption capacity between the two ions was because Cu^{2+} has smaller hydrated ionic radius compared to that of Co^{2+} and thus was able to adsorb more on AC.
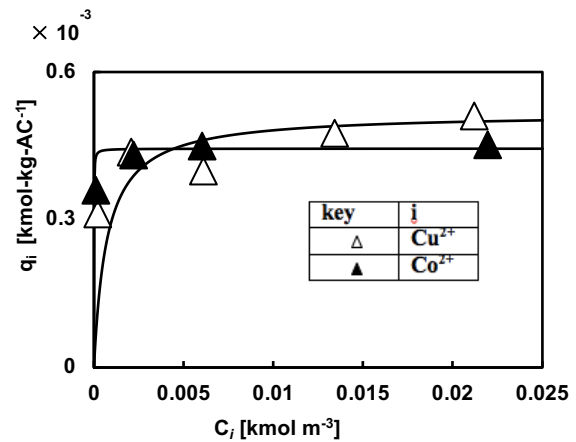
Fig. 10 Comparison of adsorption isotherms of Cu^{2+} and Co^{2+}

Table 5 shows results of saturated adsorption amounts of Cu^{2+} and Co^2 using ACs prepared by fixing C_p at 2 kmol m^{-3} but varying T and t. In all cases, the saturated

adsorbed amounts were increased with A. This is because amount of adsorption was mainly affected by A. As such, the higher the A, the higher the saturated adsorbed amount, q^*_i.

Table 5 Saturated adsorbed amount of Cu^{2+} and Co^{2+} in relation to AC surface area

AC	T [K]	t [h]	A [m²kg⁻¹]	q^*_{Cu2+} [Kmol-Kg⁻¹]	q^*_{Co2+} [Kmol-Kg⁻¹]
1	673	2	1496×10³	2.2×10⁻⁴	3.0×10⁻⁴
2	873	2	1718×10³	5.2×10⁻⁴	4.4×10⁻⁴
3	1073	2	1553×10³	4.1×10⁻⁴	3.0×10⁻⁴
4	873	0.5	1553×10³	2.4×10⁻⁴	3.6×10⁻⁴
5	873	1.0	1605×10³	3.5×10⁻⁴	3.9×10⁻⁴

3.4. Comparison between AC adsorption capacity and metal amount in real mine wastewater

Using 500m³ per day as effluent flow rate from by Zambia's largest mine, Konkola Copper Mine (KCM) and sawdust density of 210 kg m⁻³, Table 6 and 7 were obtained. **Table 6** show the Cu^{2+} and Co^{2+} that are discharged by KCM per year while **Table 7** shows the Cu^{2+} and Co^{2+} that can be removed from the discharged effluent using activated carbon produced by using all the sawdust generated on the Copperbelt province alone. With an exception of Cu^{2+} concentration, under worst case scenario, the amount of Cu^{2+} and Co^{2+} that is discharged by the mine per year was much lower than the total amount of ions that can be adsorbed using AC produced from locally available PSD. This indicated that it is possible to remove all the Cu^{2+} and Co^{2+} from the mine effluent using locally available waste sawdust and thus simultaneously solve the two earlier identified environmental challenges of the Copperbelt province

4. Conclusion

This study has demonstrated that high quality AC can be prepared from Zambia's waste and abundant pine sawdust using chemical activation. The prepared AC could adsorb and remove Cu^{2+} and Co^{2+} ions from model wastewater. The adsorption isotherms of these ions followed Langmuir model and the saturated adsorbed amounts were increased with increase in specific surface area of AC. The data thus obtained maybe helpful for designing and establishing a continuous treatment plant for wastewater enriched in heavy metals.

Nomenclature

t_c: contact time during adsorption [h],T_{wb}: water bath temperature during adsorption[K],f: speed of shaker [strokes h⁻¹],C_i : concentration of metal i in liquid at equilibrium [kmol m⁻³], $C_{i,0}$: concentration of metal i liquid at initial [kmol m⁻³],K_{Li} : Langmuir constant [m³ kmol⁻¹],Vo: Volume of liquid [m³],Y_i : fractional removal of metal i [-],Y: yield   of AC,S_{AC}: mass of activated carbon after washing and drying [kg], S_{PSD}: mass of raw

pine sawdust [kg], M_s: mass ratio of the carbon after TGA [-], S_{TGA}: mass of PSD after TGA [kg],T_{TGA} : temperature used in thermogravimetric analysis [K],C_p : concentration of phosphoric acid [kmol⁻³] A : specific surface area of AC[m² kg⁻¹],V_{mp} : micropore volume of AC [m³ kg⁻¹],V_p : amount of total pore volume that is less than d_p[cc.g-AC-1.n m⁻¹],d_p : pore diameter [nm]

Table 6 KCM Wastewater concentration

Heavy metal	Plant Condition	Metal Concentration in effluent [ppm]	Metal concentration discharged per year [kmol]
Copper	normal	15	430.79
	worst case	150	4307.90
Cobalt	normal	6	185.91
	worst case	12	371.82

Source: KCM

Table 7 Sawdust, AC and absorbable amount of Cu^{2+} and Co^{2+} from kCM

Description		Annual amount
Amount of sawdust generated [kg]		6510 ×10³
Amount of PSD-AC that can be produced [kg]		2740.71×10³
Amount of metal ions that can be adsorbed from mine effluent [kmol]	Cu^{2+}	1,414.2
	Co^{2+}	1,217.87

References

[1] Foil Vedanta, How KCM is killing the Zambian Copperbelt.,2016, pp.5-7.

[2] Mwango, A. and Kambole, C., Engineering Characteristics and Potential Increased Utilisation of Sawdust Composites in Construction—A Review. *Journal of Building Construction and Planning Research*, 2019,vol.3, pp.59-88.

[3] Mukosha, L., Onyango, M.S., Ochieng, A. and Kasaini, H., Development of better quality low-cost activated carbon from South African Pine tree sawdust: characterization and comparative phenol adsorption, no. 79, 2013, pp. 1136.

[4] Othaman., Lim, K., Konishi, S., Sato, M., Shi,N. and R. Egashira.,2008, pp. 1149–1158.

[5] Gao, X., Wu, L., Li, Z., Xu, Q., Tian, W. and Wang, R., Preparation and characterization of high surface area activated carbon from pine wood sawdust by fast activation with H 3 PO 4 in a spouted bed. *2018*, pp.925-936.

[6] Jagtoyen, M. and Derbyshire, F., Activated carbons from yellow poplar and white oak by H3PO4 activation. *Carbon*, 1998, vol.*36*, pp.1085-1097.

[7] Bouchemal, N., Belhachemi, M., Merzougui, Z. and Addoun, F., The effect of temperature and impregnation ratio on the active carbon porosity. 2009, vol.10, pp.115-120.